

FRP strengthening of RC columns for seismic retrofitting

T. Yamamoto

Technological Research Center of Tokyu Construction Co., Ltd, Sagami-hara, Japan

ABSTRACT: An experimental study was conducted to develop a strengthening method for existing reinforced concrete columns using FRP (Fiber Reinforced Plastics). Two kinds of tests were performed to clarify the effect of FRP strengthening on uniaxial concrete strength and shear-flexural behaviors of existing RC columns. The uniaxial strength of FRP-strengthened concrete increased in proportion to the FRP strengthening ratio, so that experimental equations were obtained for estimating the strength of FRP-strengthened concrete. A stress-strain relationship model for FRP-strengthened concrete was also developed. The strength and ductility of FRP-strengthened existing RC columns were considerably improved. From the tests results the requirements of reinforcing FRP ratio for strengthening existing RC columns were stated.

1 INTRODUCTION

Many existing buildings constructed in seismic zones are inadequate to current structural requirements. If those structures are not retrofitted, they might be damaged by large earthquakes. It is necessary to strengthen those structures efficiently and economically. An experimental study was conducted to develop a strengthening method for existing RC columns using FRP (Fiber Reinforced Plastics). The strength of FRP is higher than that of steel, and FRP can be easily formed into every shape. Accordingly the use of FRP combines advantages of efficiency and economy. Though some seismic retrofitting methods for existing RC buildings are reported (Kawamata 1980, Sugano 1982, Badoux 1990, etc.), there is little information on seismic behaviors of FRP-strengthened RC members. In this study two kinds of tests were performed to clarify the effect of FRP strengthening on uniaxial concrete strength and shear-flexural behaviors of existing RC columns.

2 UNIAXIAL TESTS

2.1 Specimens

Uniaxial loading test specimens are shown in Fig.1. Three types of specimens are used; 10 φ x20cm, 15 φ x30cm and 10x10x20cm. In series I, specimens were strengthened whole side by FRP. In series II, specimens were strengthened either whole side or spaced side by FRP.

2.2 Materials

In series I, the strength of concrete was 20.9MPa and 20.3MPa for 10 φ and 15 φ, respectively. In series II, the strength of concrete was 28.2MPa. The mechanical properties of FRP are shown in Table 1. FRP was made by hand lay-up technique using either carbon or glass fiber and epoxy resin. The thickness of FRP was about 0.6mm to 1.0mm.

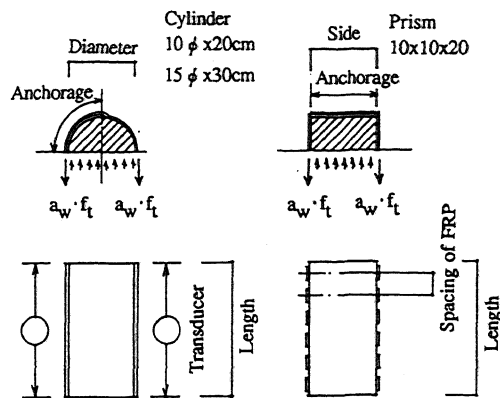


Figure 1 Specimen (Cylinder, Prism)

Table 1. Properties of FRP

FRP	Fiber	Form Layer	Thickness (mm)	ft (MPa)	E (GPa)	Young's modulus (GPa)
GFRP	Glass	Cloth 1	1.3	366	-	
GFRP	Glass	Tape 2	0.6	144	12.3	
CFRP	Carbon	Tape 2	1.0	752	78.0	

2.3 Testing procedure

Uniaxial load was applied by the 1960KN universal testing machine. The vertical strains were measured with displacement transducers along the whole length of the specimens.

2.4 Tests results

Tests results are shown in Table 3 and Table 4. Maximum strength of concrete versus the amount of strengthening FRP is shown in Fig.2. The strength of FRP-strengthened concrete increased up to three times as much as that of non-strengthened ones. Richart (1928) showed that the strength of concrete at confining stress was expressed as the following equation.

$$f_p = f_c + k \sigma_p \quad (1)$$

where

f_p = concrete strength at confining stress

f_c = non-confined concrete strength

k = coefficient

σ_p = confining stress

The confining stress induced by FRP is expressed as follows.

$$\sigma_p = 2a_w x ft / (s x D) \quad (2)$$

where

a_w = sectional area of FRP

ft = tensile strength of FRP

s = spacing of FRP

D = diameter of cylinder or long side of prism

The increment of strength was in proportion to the FRP strengthening ratio, so that experimental equations (3) - (8) were obtained for estimating the strength of FRP-strengthened concrete. Coefficient k was estimated to be 3.4 for cylinders(series I), 3.5(series II) and 0.63 for prisms respectively, by the least squares method. Since the sides of prisms can easily be dilated, FRP could not confine prisms effectively.

Relationship between strains at certain strengths and the amount of strengthening FRP are shown in Fig.3. There exists strict relationships between strains at certain stresses and lateral confinement due to FRP strengthening, too.

2.5 Uniaxial stress-strain relationship

Simplified uniaxial stress-strain relationship models for FRP-strengthened concrete were developed. A schematic diagram of stress-strain relationship is shown in Fig.4.

A-B; non-strengthened concrete stress-strain curve

B-C; C is represented by equation either (3) or (4) for stress and equation (6) for strain.

C-E; D is represented by equation (7) then take, E, on the extension of the line at cross point of 0.2 f_p .

Table 2. Tests results (Series I)

No.	Shape (mm)	Fiber	Form	Lay-er	Impreg-nation	σ_p (MPa)	f_p, f_c (MPa)	ϵ_{up} (%)	ϵ_{50p} (%)
1	100 ϕ	Glass	Cloth	1	Whole	8.92	45.3	3.00	3.90
2	100 ϕ	Glass	Cloth	1	Whole	8.92	48.7	3.58	3.93
3	100 ϕ	Glass	Cloth	1	Whole	8.92	51.4	2.58	3.40
4	100 ϕ	Glass	Cloth	2	Whole	17.8	77.5	5.63	6.75
5	100 ϕ	Glass	Cloth	1	Anchorage	8.92	26.6	1.60	1.93
6	100 ϕ	Glass	Cloth	1	Anchorage	8.92	24.1	1.35	1.90
7	150 ϕ	Glass	Cloth	1	Whole	5.98	36.4	2.10	3.08
8	150 ϕ	Glass	Cloth	1	Whole	5.98	38.2	2.28	2.95
9	150 ϕ	Glass	Cloth	1	Whole	5.98	31.8	1.02	1.95
10	150 ϕ	Glass	Cloth	2	Whole	11.9	51.3	3.12	4.23
11	150 ϕ	Glass	Cloth	1	Anchorage	5.98	21.8	0.25	1.48
12	150 ϕ	Glass	Cloth	1	Anchorage	5.98	21.9	0.23	1.35
13	100 ϕ	-	-	-	-	-	20.9	0.26	0.54
14	150 ϕ	-	-	-	-	-	20.3	0.29	0.61

ϵ_{up} : Strain at ultimate strength

ϵ_{50p} : Strain at 50% ultimate stress descending branch

Table 3 Tests results (Series II)

No.	Shape (mm)	Fiber	Form	Lay-er	Spacing (mm)	σ_p (MPa)	f_p, f_c (MPa)	ϵ_{up} (%)	ϵ_{50p} (%)
1	100 ϕ	Glass	Cloth	1	Whole	8.92	59.9	3.78	5.18
2	100 ϕ	Glass	Cloth	2	Whole	17.8	82.5	5.60	6.55
3	100 ϕ	Glass	Tape	4	@35	2.45	32.7	1.18	1.38
4	100 ϕ	Glass	Tape	4	@35	2.45	30.4	1.00	1.50
5	100 ϕ	Glass	Tape	4	@50	1.76	25.2	0.95	1.33
6	100 ϕ	Glass	Tape	4	@50	1.76	28.2	0.35	1.13
7	100 ϕ	Glass	Tape	4	Whole	3.43	32.1	1.33	1.55
8	100 ϕ	Carbon	Tape	2	@35	9.51	54.1	2.33	2.63
9	100 ϕ	Carbon	Tape	2	@35	9.51	57.6	2.65	3.50
10	100 \square	Glass	Cloth	1	Whole	8.92	29.6	0.43	5.20
11	100 \square	Glass	Cloth	2	Whole	17.8	37.8	5.98	6.43
12	100 \square	Glass	Tape	4	@35	2.45	28.4	0.38	1.07
13	100 \square	Carbon	Tape	2	@35	9.51	30.0	0.48	2.50
14	100 ϕ	-	-	-	-	-	28.2	0.30	0.52

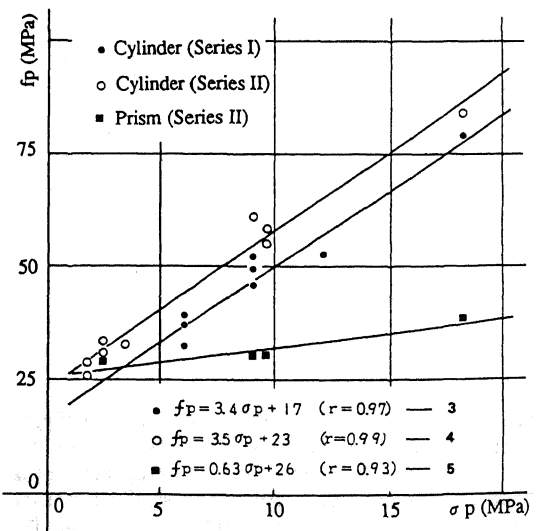


Figure 2. Ultimate strength of concrete vs. amount of strengthening FRP

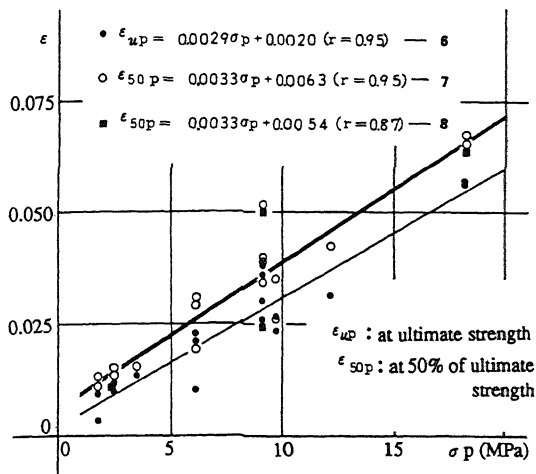


Figure 3. Strains at certain strength vs. amount of strengthening FRP

E-E; 0.2 fp constant

An example of load-deformation relationship is shown in Fig.5. It can be seen that the presented stress-strain relationship model represents whole load-deformation curves of FRP strengthened concrete.

3 SHEAR-FLEXURAL TESTS

3.1 Specimens

Five 1/4 scale column specimens were used. The specimens shown in Fig.6 and Table 4 have a cross section of 25cmx25cm, 100cm length, 0.61% (3-D13) reinforcing steel ratio, and insufficient 0.08% (4 φ -12.5cm) lateral reinforcing ratio. The lateral reinforcing ratio is about the average of existing RC columns constructed in Japan before 1960's. Specimen No.2 is strengthened by CFRP (carbon fiber), and Specimen No.3 is strengthened by GFRP (glass fiber). Specimen No.4 is sufficiently reinforced with hoops. Specimen No.5 is strengthened different wire-mesh and concrete binding method to compare with FRP strengthening method.

3.2 Strengthening method

1. FRP and mesh reinforcing ratio (Pw2) is calculated from the following equations (Arakawa 1960 and AIJ 1988, 1990) under the condition $Q_{u,min} > MQ_u$.

$$Q_{u,min} = \left\{ \frac{0.092 k_u \cdot k_p (180 + F_c)}{\frac{M}{Q \cdot d} + 0.12} + 2.7 \sqrt{p_{w1} \cdot \sigma_{y1} + p_{w2} \cdot \sigma_{y2} + 0.1N/bD} \right\} b \cdot j \quad (9)$$

where

$Q_{u,min}$ = minimum shear strength

K_u = correction factor related to effective depth of cross section

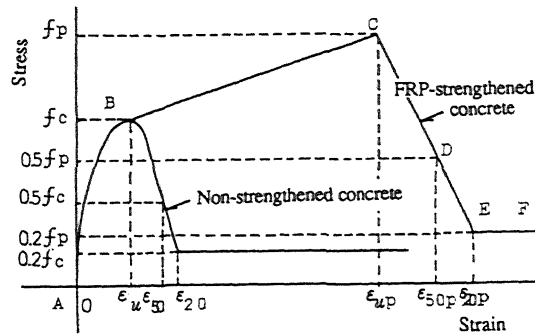


Figure 4. A schematic diagram of stress-strain relationship

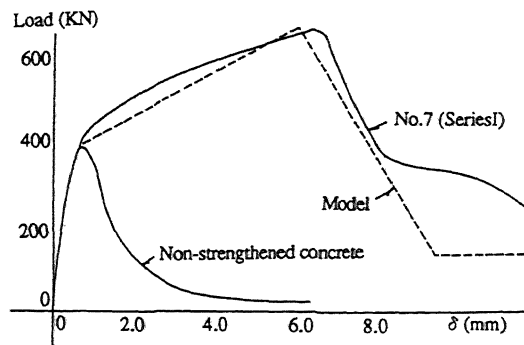


Figure 5. An example of load-deformation relationship

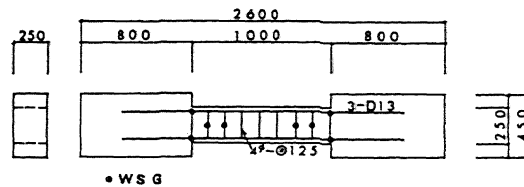


Figure 6. Column specimen

Table 4. Column specimen

Specimen	Pt	Hoop (%)	Pw1 (%)	Strengthening method	Pw2 (%)
No.1	0.61	4 φ -@125	0.08	-	-
No.2	0.61	4 φ -@125	0.08	CFRP	0.08
No.3	0.61	4 φ -@125	0.08	GFRP	0.24
No.4	0.61	6 φ -@45	0.50	-	-
No.5	0.61	4 φ -@125	0.08	Mesh&Concrete	0.20

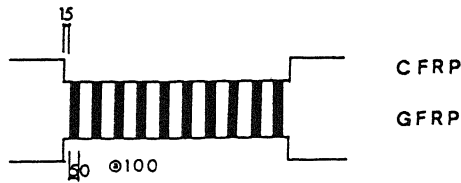


Figure 7. FRP reinforcing method

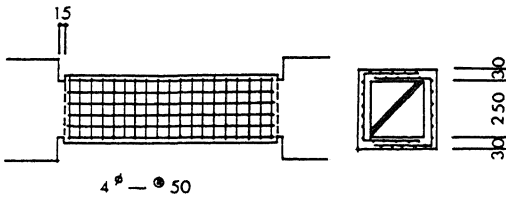


Figure 8. Mesh and concrete binding method

- K_p = correction factor related to tension reinforcement ratio
 F_c = compressive strength of concrete
 M = moment
 Q = shear force
 d = effective depth
 P_{w1} = ratio of shear reinforcement
 σ_{y1} = yield strength of shear reinforcement
 P_{w2} = ratio of FRP or mesh shear reinforcement
 σ_{y2} = yield strength of FRP or mesh shear reinforcement
 N = forced axial load normal to cross section
 b = width of cross section
 D = depth of cross section
 j = effective depth

$$M_{Qu} = \frac{M_u}{a} \quad (10)$$

where

- m_{Qu} = shear force at ultimate moment
 M_u = ultimate moment
 a = shear span

$$M_u = 0.8 a_t \sigma_y D + 0.5 N D \left(1 - \frac{N}{b D F_c} \right) \quad (11)$$

where

- a_t = area of tension reinforcement
 σ_y = yield strength of tension reinforcement

2. Reinforcing FRP was made by hand lay-up method using 50mm-wide woven fiber tape and epoxy resin. The method of FRP reinforcing is shown in Fig.7. Mesh and concrete binding method is shown in Fig.8. Reinforcing meshes were formed into channel shape and gathered to bind existing RC columns.

3.3 Materials

The properties of steel, concrete and FRP are shown in Table 5, 6 and 7. The strength of concrete was 21.1MPa and Young's modulus was 16.5GPa. The strengths of CFRP and GFRP were 752MPa, 119MPa, respectively

Table 5. Properties of steel

Steel	Diameter (mm)	f_y (MPa)	f_t (MPa)	Use
D13	13	358	521	Longitudinal bar
6 ϕ	6	426	531	Hoop : Specimen No.4
4 ϕ	4	439	585	Hoop
Mesh 4		447	639	Binding mesh : Specimen No.5

Table 6. Properties of concrete

Concrete	f_c (MPa)	Young's modulus (GPa)	Testing age (days)
Column	21.1	16.5	180
Strengthen	27.6	23.8	40

Table 7. Properties of FRP

FRP	Fiber	Form Layer Thickness (mm)	f_t (MPa)	Young's modulus (GPa)
CFRP	Carbon Tape	2	1.0	752
GFRP	Glass Tape	10	3.0	119

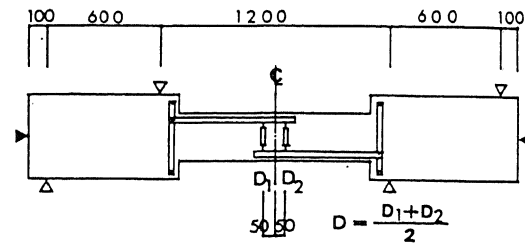


Figure 9. Loading and measurement method

and Young's modulus were 78.0GPa, 13.1GPa, respectively.

3.4 Seismic loading

The loading and measurement method are shown in Fig.9. The specimens were subjected to shear force by the 1960KN universal testing machine while constant axial load was applied by the 4-PC bars. 3.92MPa axial stress which is the average stress of existing first story column in low-rise buildings was applied. The shear force was applied under the control of the relative displacement angles between top and bottom of the column; five cycles at 1/200, 1/100, 1/50 and single cycle at 1/20. The loading history is shown in Fig.10.

3.5 Measurement

The axial load was measured with load cells and controlled within 3% deviation from the initial applied load. Two displacement transducers were used to measure the relative displacements between the stabs and to check the balance of the both stab rotations. Strains of longitudinal bars, hoops and FRP in the hinge zone were measured with strain gauges.

Table 8. Shear-flexural tests results

Specimen	Strength-ening	Rigidity		Cracking		Cracking		Strength		Strength		Displacement Ultimate	Failure Mode		
		Initial (KN/mm)	(Ke/Ki) (KN/mm)	Yielding (Ke/Ky) (KN)	Flexural (Qe/Qf) (KN)	Shear (Qe/Qs) (KN)	Yielding (Qe/Qy) (KN)	Ultimate (Qe/Qu) (KN)							
No.1	-	36.3	0.90	10.2	0.88	19.6	0.58	68.6	1.21	104	1.17	112	1.14	1/50	Shear
No.2	CFRP	33.8	0.84	11.6	1.00	19.6	0.58	80.4	1.41	108	1.22	114	1.16	≥1/12.5	Flexure
No.3	GFRP	35.6	0.89	10.9	0.94	19.6	0.58	68.6	1.21	105	1.19	119	1.21	1/18	FRPbraking off
No.4	Foop	37.2	0.93	12.3	1.07	24.5	0.72	78.4	1.38	104	1.17	114	1.16	≥1/12.5	Flexure
No.5	Mesh	43.2	1.07	13.9	1.20	29.4	0.87	114	1.88	108	1.22	118	1.20	≥1/12.5	Flexure

Ke: Measured rigidity, Ki: Calculated rigidity obtained from elastic theory, Ky: Calculated rigidity obtained from AIJ Standard (1988)
 Qe: Measured shear strength, Qf, Qs, Qy, Qu: Calculated cracking or yielding or ultimate strength obtained from AIJ Standard (1988)

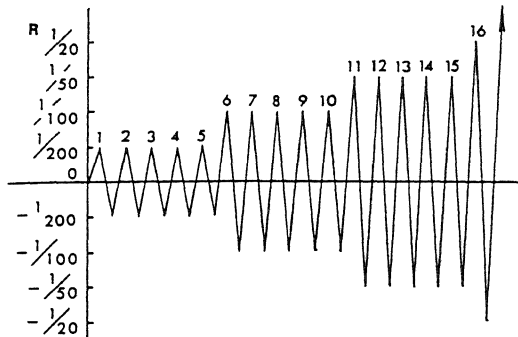


Figure 10. Loading history

3.6 Tests results

Tests results are shown in Table 8. Load-displacement relationships are shown in Fig.11. Cracking patterns of specimens at failure are shown in Fig.12.

3.6.1 Failure process

With the increase of shear force, flexural cracks occurred at both column ends in the 1st cycle, and then shear cracks occurred. After that the longitudinal bars of columns yielded. Specimen No.1 failed suddenly in the 3rd cycle at the relative displacement angle 1/50 due to occurrence of wide diagonal shear crack connecting two column stabs. The other specimens, after cyclic loading at the relative displacement angle 1/50, endured up to the relative displacement angle 1/20 and the load-displacement behaviors were stable. Over the relative displacement angle 1/20, the specimens were forced to deform to the relative displacement angle 1/12.5. Specimen No.2, No.4 and No.5 did not collapse finally. While Specimen No.3 collapsed at the relative displacement angle 1/18 due to FRP braking off at column ends.

3.6.2 Cracking strength

Flexural cracking loads were 19.6KN to 34.3KN and lower than those of calculated loads. Shear cracking loads were 68.6KN to 114KN and higher than those of calculated loads. Except Specimen No.5 which had a wider concrete section, shear cracking loads were almost the same.

3.6.3 Rigidity and flexural strength

The initial rigidity of specimens before cracking were about the same, while the initial rigidity of Specimen No.5 was 1.2 times larger than those of the other specimens. The rigidity at yielding of non-strengthened Specimen No.1 was the lowest and that of Specimen No.5 was the highest. The flexural strengths were almost the same among the specimens, since there was no increase of effective depth of the strengthened specimens even in Specimen No.5. From the standpoint of seismic retrofitting it is desirable that the existing RC columns are strengthened without increasing any flexural strength.

3.6.4 Ultimate shear strength and deformation

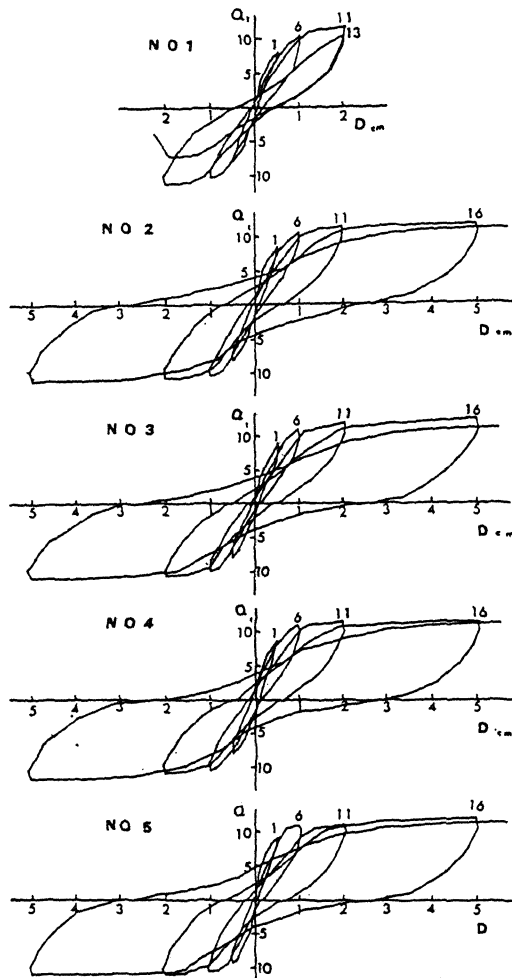
The measured maximum strength exceeded about 10% for calculated strength obtained from equation (2). It is assumed that the ultimate deformation is the 20% load decrement point to the maximum load at the same cycle before relative displacement angle 1/50 and after that to the maximum load experienced. The ultimate relative displacement angles of specimens were 1/50 for Specimen No.1, 1/18 for Specimen No.3 and over 1/12.5 for the other Specimens.

3.6.5 Strains of longitudinal bars, hoops and FRP

The longitudinal bars of the specimens yielded at about relative displacement angle 1/200. The hoops of Specimen No.1 yielded at the relative displacement angle 1/50, and that of No.3 and No.5 reached yield strain at the relative displacement angle 1/20. The hoops of Specimen No.2 and No.4 reached yield strain over that displacement angle. At the relative displacement angle 1/20 FRP strains were 2000μ, 4000μ for Specimen No.2, No.3, respectively. FRP strains were slightly larger than that of hoops at the same sections. Final CFRP strains at relative displacement angle 1/12.5 were about 3000μ near the column ends.

3.6.6 FRP strengthening ratio

FRP strengthened specimens behaved ductile in cyclic loading, and inner hoops and outer strengthening FRP worked together. Consequently it was realized that equation (9) held true for estimating FRP strengthening ratio. In equation (9), yield strength was used 0.7 of tensile strength for CFRP and 1.0 of tensile strength for



Superscription represents number of loading

Figure 11. Load-displacement relationships

GFRP. Considering the ultimate deformations of specimens and the brittle behavior of FRP, it is preferable to use 0.7 of FRP tensile strength in equation (9) for estimating FRP strengthening ratio of existing RC columns.

4. CONCLUSIONS

The following conclusions are derived from the tests results described in this paper.

1. It was realized that FRP strengthening could significantly improve the strength and ductility of existing RC columns efficiently and economically.
2. The uniaxial strength of FRP-strengthened concrete increased up to three times as much as that of non-strengthened ones in proportion to the FRP strengthening ratio. Experimental equations were obtained for estimating the strength of FRP-strengthened concrete.
3. Uniaxial stress-strain relationship models for FRP-

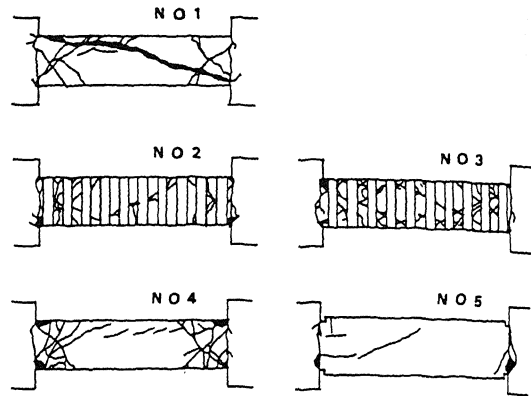


Figure 12. Cracking pattern of specimens at failure

strengthened concrete were developed. They were in good agreement with tests results.

4. Shear-flexural tests showed that the ductility of strengthened columns was considerably improved. While non-strengthened column collapsed at the relative displacement angle of 1/50, FRP-strengthened columns endured up to 1/12.

5. It can be seen that inner hoops and strengthening outer FRP worked together. And equation (9) held true for estimating FRP strengthening ratio. Considering the ultimate deformations of specimens and the brittle behavior of FRP, it is preferable to use 0.7 of FRP tensile strength in equation (9) for estimating FRP strengthening ratio of existing RC columns.

REFERENCES

- AIJ. 1988. Standard for Structural Calculation of Reinforced Concrete Structures : Architectural institute of Japan.
- AIJ. 1990. Ultimate strength and deformation capacity of buildings in seismic design : Architectural institute of Japan.
- Arakawa, T. 1960. A study on shear strength of reinforced concrete beams : Transactions the architectural institute of Japan, vol.66 : 437-440.
- Badoux, M., and Jirsa, J.O. 1990. Steel bracing of RC frames for seismic retrofitting : Journal of structural engineering, vol.116, No.1 : 55-74.
- Kawamata, S., and Masaki, Q. 1980. Strengthening effect of eccentric steel braces to existing RC frames : Proc., seventh world conf. on earthquake enrg, Istanbul, Turkey.
- Sugano, S. 1982. An overview of the state-of-the-art in seismic strengthening of existing reinforced concrete buildings in Japan : Proc.,third seminar on repair and retrofit of structures., Ann Arbor, Mich. : 328-349.
- Richart, F.F., Brandtzaeg, A., & Brown, R.L. 1928 A study of the failure of concrete undercombined compressive stress : Bulletin No.185, Univ. of Illinois eng. experiment station, Urbana.